Biological Psychology 196 (2025) 109016

Contents lists available at ScienceDirect

Biological Psychology

journal homepage: www.elsevier.com/locate/biopsycho

EEG evidence for spatial selectivity in feature-based preparation for visual search

Gordon Dodwell [1,*], Rebecca Nako [2], Martin Eimer [3]

School of Psychological Sciences, Birkbeck, University of London, Malet Street, Bloomsbury, London WC1E 7HX, UK

ARTICLE INFO

Dataset link: EEG evidence for spatial selectivity in feature-based preparation for visual search

Keywords:
EEG
Event-Related Potentials (ERP)
Visual Attention
Attentional control
Spatial
Selection
Visual Search
Attentional Templates
N2pc component

ABSTRACT

In many visual search tasks, the detection of target objects in visual search requires feature-selective attentional guidance and space-based attentional selection. Feature-based attention is often assumed to operate in a spatially global fashion across the entire visual field, but there is also evidence that it can be restricted to task-relevant locations under some conditions. Here, we investigated whether such spatial filtering processes are already evident when representations of target-defining features (attentional templates) are activated during the preparation for an upcoming search episode. We measured N2pc components (an electrophysiological index of attentional allocation) in response to a rapid series of lateral task-irrelevant but template-matching colour probes that appeared while participants prepared for an upcoming search task with colour-defined targets. Critically, search targets would either always appear in the same lateral regions of visual space as the probes, or at different locations (near fixation or in lateral areas that never contained probes), thus rendering the probed locations either task-relevant or irrelevant. N2pc components triggered by target-colour probes during the preparation period emerged later and were attenuated when probes were presented at irrelevant locations. This demonstrates that the effects of preparatory feature-based attentional templates can be modulated by spatial expectations. However, this type of spatial filtering during search preparation only attenuates but not completely eliminates feature-based attentional modulations.

1. Introduction

Space-based and feature-based attention are two key mechanisms that facilitate selectivity in visual processing. In many situations, both are required to ensure that attention is allocated adaptively to objects and events that are currently relevant. A common example is in visual search, where observers search for a specific target object amongst multiple distractors, without prior knowledge of the target's location. Here, attention is assumed to be first guided towards all objects with target-matching features, before one or more of these objects are spatially selected for further processing (e.g., Wolfe, 2021; see also Bichot, Rossi, & Desimone, 2005). During visual search, feature-based attention is controlled by representations of target-defining attributes ("attentional templates"; Duncan & Humphreys, 1989; Olivers, Peters, Houtkamp & Roelfsema, 2011), which are believed to be stored in working memory and can be activated prior to the presentation of visual search displays (e.g., Desimone & Duncan, 1995; Grubert & Eimer, 2018). These templates act by selectively enhancing neural activity in response to visual objects with task-relevant features, thereby biasing the subsequent allocation of spatial attention towards these objects (see Eimer, 2014, 2015, for further details).

During visual search for known targets at unknown locations, feature-based attention precedes and controls the space-based selection of particular objects. However, feature-based and space-based attention could also operate in parallel under certain circumstances. In search tasks where target objects only appear within specific regions of the visual field, it would be useful if biases of visual processing triggered by feature-based attention were spatially selective and could be restricted to these task-relevant locations. Evidence for efficient spatial filtering has been found in visual search studies that investigated attentional capture by irrelevant objects with abrupt onsets (e.g., Yantis & Jonides, 1990) or colour singletons (Theeuwes, Kramer, & Atchley, 2001). These

* Corresponding author.
E-mail addresses: g.dodwell@bbk.ac.uk (G. Dodwell), r.nako@bbk.ac.uk (R. Nako), m.eimer@bbk.ac.uk (M. Eimer).
[1] orcid.org/0000–0001-6772–9849
[2] orcid.org/0000–0003-1073–414X
[3] orcid.org/0000–0002-4338–1056

https://doi.org/10.1016/j.biopsycho.2025.109016
Received 22 November 2024; Received in revised form 4 February 2025; Accepted 15 March 2025
Available online 21 March 2025

salient distractors fail to capture attention when their location is known in advance, indicating that spatial filtering can limit the allocation of spatial attention to particular regions in the visual field ("attentional windows"; Theeuwes, 2010). However, it remains unclear whether feature-based attention can be restricted in similar ways in other types of search tasks. In fact, it is often assumed that feature-based attention always operates in a spatially global fashion – that is to say, across the entire visual field, even at locations that are known to be task irrelevant (e.g., Störmer & Alvarez, 2014; see also Liu, 2019, for a review). Evidence for this assumption comes from research using single-cell recordings (e.g., Martinez-Trujillo & Treue, 2004), fMRI (e.g., Serences & Boynton, 2007), event-related brain potentials (Zhang & Luck, 2011), and steady-state visual evoked components (SSVEPs; e.g., Andersen, Hillyard, & Müller, 2013; Störmer & Alvarez, 2014; Forschack, Andersen, & Müller, 2017). These studies used variations of a general procedure that involves observers continuously monitoring visual input in one region of visual space (e.g., in one hemifield) in order to detect target events defined by a particular feature (e.g., colour or movement direction). Although stimuli at other locations could be entirely ignored, visual activity triggered by these stimuli was consistently enhanced when they matched the target-defining feature (but see Andersen & Hillyard, 2024, for recent SSVEP evidence that the onset of these modulations is delayed in the unattended visual field). Overall, these observations suggest that feature-based attention effects are indeed spatially global, and thus cannot be eliminated by spatial filtering.

In many visual search tasks, where the location of an upcoming target stimulus among distractors is entirely unpredictable, it would indeed be adaptive for feature-based attentional guidance to operate in a spatially global manner. However, it would be surprising if feature-based guidance were always entirely unaffected by knowledge of the limitations on where task-relevant objects could appear. It is important to note that the presence of feature-based attentional modulations at irrelevant locations does not, in itself, demonstrate the absence of spatial filtering. Some degree of spatial selectivity may still be operational, even if it only attenuates, rather than completely eliminates, the effects of feature-based attention. In support of this idea, it has been shown that visual processing enhancements triggered by stimuli with target-matching features are stronger at potentially relevant as compared to irrelevant locations (e.g., Martinez-Trujillo & Treue, 2004; Andersen, Fuchs, & Müller, 2011), and decrease with increasing distance to task-relevant locations (Leonard et al., 2015; see also Berggren & Eimer, 2020, for an ERP study where such effects were strongly attenuated or entirely absent for stimuli in the task-irrelevant hemifield).

Previous research investigating the impact of spatial filtering on feature-based attention and guidance in visual search and other attentional selection tasks has primarily focused on task-relevant stimulus displays. Feature-selective attention effects were measured while observers engaged in detecting and identifying a target object, or monitoring continuous visual input for the appearance of task-relevant events. However, feature-based attentional mechanisms are already activated before the presentation of relevant displays, when observers are preparing for an upcoming attentional selection task. In visual search, attentional templates for particular target features are assumed to be activated in a preparatory fashion, prior to the arrival of visual search displays (e.g., Duncan & Humphreys, 1989; Desimone & Duncan, 1995; Olivers et al., 2011; Grubert & Eimer, 2018). These search templates are assumed to represent one or more target-defining non-spatial features (such as colour, orientation, or shape). In typical search tasks where no advance knowledge about target location is available (i.e., target objects appear randomly at any search display location), search templates will not include any spatial information. However, what is not yet known is whether preparatory search templates can provide both feature-based and space-based information about upcoming search targets when these targets are known to only appear within particular regions of the visual field. If space-based attentional templates are already activated during search preparation, they could interact with feature-based templates. In this case, any feature-based attentional modulations during this period should be subject to spatial filtering, and thus be attenuated or absent at task-irrelevant locations.

The goal of the present study was to test this possibility. It is generally challenging to measure the activation of attentional templates during search preparation, because these processes occur covertly, in the absence of any directly observable behaviour. To obtain direct insights into the presence and time course of preparatory search template activation, we have recently developed a method (the *rapid serial probe presentation* procedure, or *RSPP*; Grubert & Eimer, 2018, 2019, 2020; Dodwell, Nako, & Eimer, 2024a) to track these processes in real time with electrophysiological measures. In these experiments, circular search displays contained a colour-defined target together with multiple distractors in different colours. Critically, search displays were preceded by a series of task-irrelevant probe displays, each containing a colour singleton which either matched the colour of the target or a different non-target colour. These circular probe displays were presented in rapid succession, occurring every 200 ms between successive search displays. Probe singletons matching the target colour could trigger an event-related potential (ERP) marker of attentional object selection, the N2pc component (see Eimer, 1996; Hickey, DiLollo, & McDonald, 2009; Luck & Hillyard, 1994; Woodman & Luck, 1999). The presence of an N2pc to a particular probe demonstrates that it captured attention in a task-set contingent fashion (see Folk et al., 1992; Eimer and Kiss, 2008), implying that a corresponding target-colour search template was active at the moment the probe was presented. Reliable probe N2pcs were only observed during the final 800 ms of the preparation period, but not earlier, and were largest immediately prior to search display onset. This temporal pattern indicated that target template activation processes were triggered anew on each trial and were sensitive to temporal expectations about the arrival of the next task-relevant search display. Importantly, no N2pcs were triggered at all by probe singletons appearing in a non-target colour, demonstrating that these components indeed reflected colour-selective preparatory search template activation, and not any salience-driven attentional capture triggered by colour singletons regardless of their task relevance.

The singleton probe procedure used in these previous experiments successfully tracked the presence and time course of preparatory target colour template activation processes. However, it was not designed to directly investigate whether these templates also hold spatial information about target locations. In these experiments, the circular search displays were always presented at a larger eccentricity than the circular probe displays. The fact that target-matching singleton probes triggered reliable N2pcs even though they always appeared at nominally irrelevant locations (i.e., closer to fixation than the search targets) might suggest that search templates provide only feature-based but not location-specific information, in line with the general idea that feature-based attention operates in a spatially global fashion. However, this is by no means conclusive, since none of these previous experiments included a condition where probes appeared at locations that could be occupied by subsequent search targets. It was therefore not possible to compare N2pc amplitudes to probes at task-relevant versus irrelevant locations, in order to find out whether the activation states of feature-based attentional templates were modulated by spatial filtering. Furthermore, since the probes always appeared *inside* the region occupied by the search display stimuli, they may have been included within a unitary wide focus of spatial attention that covered all search display items.

In the present study, we employed the same general probe presentation logic, but used entirely different stimulation procedures, as illustrated in Fig. 1. Each probe display consisted of two lateral 'clouds' composed of dots in four different colours, with one of these colours matching the colour of the upcoming search target (see Methods section for details). Critically, the side on which these target-colour dots were presented was independently determined for each successive probe display, to rule out the possibility of any sequential dependencies between target-colour dot locations across individual probe displays.

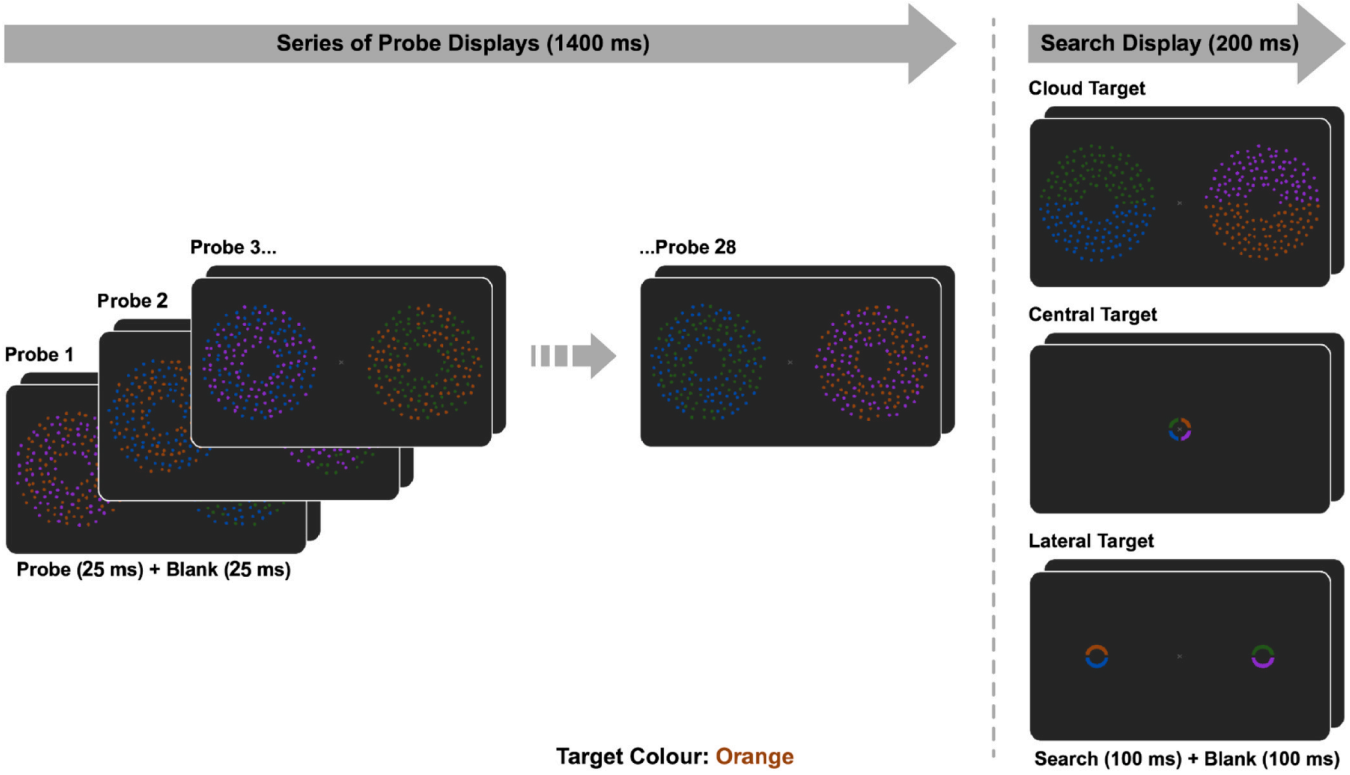

Fig. 1. Example trial sequence. A series of 28 probe displays were presented at regular 50 ms intervals, with each display remaining on screen for 25 ms followed by a 25 ms "blank" screen containing only a fixation cross. This was followed by the appearance of a search display, which was presented for 100 ms, followed by a 100 ms "blank" screen. In probe displays, two "clouds" of coloured dots were presented to the left and right of screen centre. The dots within each "cloud" were pseudo-randomly coloured to avoid producing any discernible patterns or structures. In the "Cloud Target" search displays, the same "cloud" stimuli appeared, but the dots within the upper and lower halves of each cloud were uniformly coloured, producing a discernibly "split" structure. In the "Central Target" search displays, a "ring" segmented into four coloured sections was presented at screen centre, surrounding the fixation cross. In the "Lateral Target" search displays, two separate "rings", each segmented into differently coloured upper and lower sections, were presented to the left and right of screen centre, spatially overlapping with the unpopulated centre of each "cloud" stimulus in the probe displays. Participants were tasked with responding after each search display by indicating the vertical position ("up" or "down") of a predefined target colour.

Analogously, the location of the target-colour area in the search displays was not correlated with the location of any preceding target-colour probes. This independence of the side of target-colour dots between successive displays made it possible to separately and independently compute lateralised N2pc components for each successive target-colour probe and the search target, even though displays were presented in rapid succession, resulting in substantial temporal overlap of non-lateralised ERP components. The probe displays were presented every 50 ms, and N2pc components were computed independently for each probe display by comparing ERPs triggered contralateral versus ipsilateral to the side where the target-colour set of dots were present, to track the time course of search template activation processes. Dots in the probe displays matching the target colour were expected to attract attention (thereby triggering an N2pc) if they appeared while a corresponding search template is active. To address our main question whether these preparatory states are spatially selective (i.e., sensitive to information about possible target locations), we computed and compared probe N2pc components across three different task conditions (Fig. 1, right panels). In the "Cloud Target" condition, probes and search displays appeared at the same locations, thus rendering probe locations task-relevant. Search displays included four semicircular areas in four different colours, with one designated as target colour. In the other two task conditions, the locations of the coloured "cloud" probes were task-irrelevant. In the "Central Target" condition, search displays included a ring composed of four differently coloured segments at the screen centre. In the "Lateral Target" condition, search displays included two rings with differently coloured upper and lower segments in the left and right visual field, occupying the empty inner area of each cloud (see Fig. 1). Task instructions were the same in all three tasks: Participants had to report the vertical location (upper versus lower visual field) of the target-coloured area/segment in the search displays.

The Cloud Target condition employed here was already included in another recent study where the new cloud probe procedure described above was first introduced (Dodwell, Nako, & Eimer, 2024b). In this study, clear probe N2pc components were obtained contralateral to target-colour dots. This demonstrates that despite the very rapid presentation rate of individual cloud probes and the fact that both lateral clouds had to be monitored simultaneously (which could result in rapid switches of feature-based attention between clouds; see Re, Inbar, Richter & Landau, 2019, for behavioural evidence that the allocation of feature-based attention fluctuates rhythmically between stimuli), search template activation processes could still be successfully tracked. Similar to previous findings (e.g., Grubert & Eimer, 2018), significant probe N2pcs were measured during the final 800 ms prior to the onset of the next search display (but not earlier), and N2pc amplitudes increased in size towards the end of this preparation period. This pattern of results was expected to be confirmed in the Cloud Target condition of the present experiment. Importantly, this condition now served as a baseline measure of the effects of preparatory colour-selective search template activation processes at currently task-relevant locations in the visual field.

The critical new question was whether and how these effects would change in tasks where search targets are no longer presented at the locations occupied by the probe clouds. If preparatory search templates only represent target-defining non-spatial features irrespective of where targets would appear, there should not be any systematic differences in

the size and temporal pattern of probe N2pc components in the Central and Lateral Target tasks relative to the Cloud Target task. This would also be in line with the assumption that feature-based attentional control processes are not subject to any spatial filtering, and therefore modulate visual processing in a spatially global fashion. Alternatively, if preparatory processes are sensitive to information about target location, feature-selective and location-selective preparatory states should interact, resulting in some spatial filtering of colour-selective attentional modulations triggered by the probe displays. Probe N2pc components might emerge later during the preparation period during the Central and/or Lateral Target conditions, their amplitudes might be attenuated, or they could even be entirely absent. In addition, systematic differences between the Central and Lateral target conditions might also be expected. These two conditions were designed to contrast conditions where spatial filtering is either easy (Central Target) or more challenging (Lateral Target). In the Central Target condition, spatial filtering should be relatively straightforward, as attention can be fully focused near fixation, while excluding all lateral areas of the visual field. Here, colour-selective attentional templates may only affect visual processing in the foveal region, but not in the periphery where the clouds are located, resulting in the absence of any attentional capture (and N2pc components) triggered by target-colour probes. In the Lateral Target condition, search targets appear unpredictably in the left or right visual field in the unfilled centre region of a cloud, so that both of these lateral locations were equally task-relevant. Here, any spatial filtering would have to prioritize the two empty central sectors not occupied by the clouds, while excluding the surrounding areas. Effective filtering might not be possible under these circumstances, which would result in attentional capture (and reliable N2pc components) to target-colour probes that may be similar in size to the effects observed in the Cloud Target condition.

2. Materials and methods

2.1. Participants

A total of 20 participants took part in the study ($M = 24.4$ years, $SD = 6.8$ years; sixteen female, two left-handed). All participants provided written informed consent prior to the start of testing, reported normal or corrected-to-normal vision, and were monetarily compensated for their participation. The collected sample size of 20 exceeded the minimum of 19 necessary to achieve sufficient statistical power as indicated by an a priori power analysis ($\alpha = 0.05$, $1 - \beta = .80$, $f = 1.25$; G*Power; Faul, Erdfelder, Lang & Buchner, 2007). The goal of this analysis was to determine the required sample size needed to obtain reliable probe N2pc components in the task condition where we predicted that these components should be reliably present (Cloud Target condition). The effect size used in this analysis ($\eta_p^2 = 0.61$) was based on the amplitude of N2pc components triggered by target-matching colour-singleton probe stimuli, which were observed in a prior experiment (Dodwell et al., 2024b; 50 ms ISI condition) that employed exactly the same procedures as in the current Cloud Target condition. Specifically, this effect size was taken from the main effect of laterality for target-coloured probes across the final 8 probe displays (probes 21–28). Because this power analysis was based on a main effect, it does not necessarily imply that any interactions (i.e., differences in N2pc components between the Cloud Target and the other two task conditions) can also be reliably detected with the current sample size. Thus, the absence of such interactions would not provide strong evidence for the absence of task-related N2pc differences. The present study was conducted in accordance with the Declaration of Helsinki and approved by the Psychology Ethics Committee at Birkbeck, University of London.

2.2. Materials

The experiment was presented on a 24.5-inch monitor (BenQ Zowie XL2546; TN panel, 1920 × 1080 resolution, 240 Hz refresh rate) at a viewing distance of approximately 100 cm. Presentation was controlled by a Windows PC (Acer PO3–630; Intel Core i7–11700F, NVIDIA GeForce RTX 3070). The luminance of all colours employed in the study were measured directly on the experimental monitor using a high-precision luminance meter (Konica Minolta LS-100). The experimental script was coded in Python (ver. 3.9.13) using the Psychopy toolbox (ver. 2023.1.3; Peirce et al., 2019). Participants completed the experiment while seated in a dimly lit and sound-controlled cabin with electromagnetically shielded walls.

The EEG data were recorded a set of 64 active Ag/AgCl electrodes connected to a digital amplifier (ActiCAP slim/snap & BrainAmp DC; Brain Products GmbH, Gilching, Germany). 61 electrodes were placed over scalp positions according to the international 10–10 system (electrode sites: Fp: z, 1, 2 | AF: 3, 4, 7, 8 | F: z, 1, 2, 3, 4, 5, 6, 7, 8, 9, 10 | FC: 1, 2, 3, 4, 5, 6 | FT: 7, 8 | T: 7, 8 | C: z, 1, 2, 3, 4, 5, 6 | CP: z, 1, 2, 3, 4, 5, 6 | TP: 7, 8 | P: z, 1, 2, 3, 4, 5, 6, 7, 8 | PO: z, 3, 4, 7, 8 | O: z, 1, 2 | VEOG, HEOG-L, HEOG-R). Three additional electrodes were also placed over the outer canthi of each eye and the inferior orbit of the left eye, providing a means to monitor both vertical and horizontal eye movements. Electrode impedances were maintained below 10 kΩ based on ground and reference electrodes placed over scalp-sites AFz and FCz, respectively. Sampling of the raw EEG signals was performed at 1 kHz, which were digitally filtered between 0.01 and 250 Hz as they were recorded. The EEG signals and event triggers sent by the presentation computer were recorded by a Windows PC (Dell Precision 5820, Intel Xeon W-2235, NVIDIA Quadro P220) running the BrainVision Recorder software (ver. 1.25.001; Brain Products GmbH, Gilching, Germany). The delay in event timings between the presentation and recording computers was verified to be no greater than one ms.

2.3. Experimental design

The present study employed a variant of the RSPP paradigm (Dodwell et al., 2024b) in which a series of task-irrelevant probe displays were presented at regular 50 ms intervals between successive task-relevant search displays. Critically, we evaluated differential search display configurations in three separate search conditions (“Cloud Target,” “Central Target,” and “Lateral Target”), manipulating the form and spatial location of a colour-defined target. Our aim was to examine whether feature-based attentional preparation for a predefined target colour would be applied in a spatially global manner, or alternatively, would become spatially selective depending on the format of each search display configuration. If feature-based attention is spatially global, then the preparatory attentional profile captured by the RSPP procedure should remain relatively uniform across all three search display configurations. Conversely, if feature-based attention can be spatially selective, preparatory attentional profiles should differ substantially depending on whether or not the contents of the probe and target displays spatially overlap. See Fig. 1 for a depiction of a trial sequence and each potential search display.

Probe displays consisted of two clouds of coloured dots on a dark grey background (CIE $x/y = 0.285/0.347$; 5.25 cd/m^2), positioned at an eccentricity of 6.5° of visual angle to the left and right of a grey central fixation cross (0.4° × 0.4° visual angle; 0.291/0.333; 24.0 ± 0.3 cd/m^2). A cloud comprised 171 individual dots (0.25° visual angle), each randomly located along a radius (0.29° visual angle Ø) surrounding a unique anchor point. These anchor points were evenly positioned along the radii of six concentric rings (2.88°, 4.04°, 5.20°, 6.35°, 7.51°, and 8.66° visual angle Ø, respectively). In every new probe display, the positions of these dots shifted within a 120° arc directly opposite their prior position, relative to their respective anchor points. This design ensured that the dots composing each cloud could never overlap within a given display, nor exhibit any coherence or predictability of motion from one display to the next. The dots within each cloud appeared in equal proportions of two unique colours, resulting in four equiluminant

colours appearing within a given probe display (orange: 0.504/0.440, green: 0.296/0.579, blue: 0.181/0.189, purple: 0.207/0.095; all 24.0 ± 0.3 cd/m^2). Each colour could appear on only one side of the screen at any given time, providing the lateralization necessary for a predefined target colour to elicit an N2pc component. The lateral locations of the target and non-target colours were pseudo-randomized across all probe displays, ensuring their positions and pairings remained unpredictable yet counterbalanced throughout the entire experiment. The colours of specific dots within a given cloud were also pseudo-randomized in each display to avoid the formation of any discernible patterns or structures.

In the Cloud Target condition, the search display was composed of the same clouds of coloured dots and central fixation cross as in the probe displays. However, the dots appearing within the upper and lower sections of each cloud were assigned uniformly separate colours, thereby producing a discernibly "split" structure (see Fig. 1, "Cloud Target"). As such, the coloured dots in the Cloud Target search display occupied the same spatial regions as those in the probe displays. In the Central Target condition, the search display included a ring (outer edge: 2° visual angle Ø, inner edge: 1.2° visual angle Ø) bisected along the vertical and horizontal meridians by 0.3° of visual angle into four differently coloured segments. This ring was presented at screen centre surrounding the central fixation cross and was therefore entirely spatially segregated from the regions of the screen occupied by the clouds of the probe displays (see Fig. 1, "Central Target"). In the Lateral Target condition, the search display contained two separate rings (outer edge: 2° visual angle Ø, inner edge: 1.2°), bisected along the horizontal meridian by 0.3° visual angle into two differently coloured segments. These rings were presented at an eccentricity of 6.5° of visual angle to the left and right of the central fixation cross. While the lateralised rings appeared at the same eccentricity as the clouds in the probe displays, they remained spatially segregated from the clouds, having a smaller diameter than the inner-most concentric ring of the cloud array (see Fig. 1, "Lateral Target"). In all three search conditions, participants were tasked with indicating whether a predefined target colour appeared at the top or bottom of its respective cloud or ring (irrespective of its lateral position), by pressing the "up" or "down" arrow keys, respectively.

The study was divided into three sets of 24 blocks each, with each set corresponding to a different search condition and each block containing 12 trials. To eliminate any potential task order effects, the sequence of search conditions across the three sets was counterbalanced amongst participants. At the start of each block, the predefined target colour was updated pseudo-randomly and indicated to the participant in text (e.g., "The target colour is ORANGE" with the word "orange" appearing in the corresponding colour). This ensured that all four stimuli colours defined the target in 6 blocks of each search condition. Each block began with an entirely blank screen for 500 ms, followed by the appearance of the fixation cross, which was displayed for an additional 500 ms and then remained on screen until the end of the block. This was followed by a sequence of 12 trials, each beginning with a series of 28 probe displays. Every probe display remained on screen for 25 ms, followed by a 25 ms "blank" screen containing only the fixation cross. Directly following the probe series, a search display was presented for 100 ms, followed by a "blank" screen containing only the fixation cross for an additional 100 ms. The final trial in each block was followed by an additional probe sequence without a subsequent search array, ensuring visual uniformity in the response windows of each trial. Trials within a block ran consecutively without pause between the end of one trial and the start of the next. Consequently, participants provided their response to the search display of the preceding trial during the probe series of the following trial. A live visualisation of the stimulation sequence in all three search conditions can be viewed at the following URL: https://gordondodwell.github.io/RSPPHD_Spatial/.

2.4. EEG preprocessing

Processing of the EEG data was performed using MNE Python (ver. 1.7.0, Gramfort et al., 2013). The continuous data of each participant were first passed through a 0.1 Hz high-pass FIR filter and a FIR notch filter at 50 Hz intervals between 50 and 250 Hz, removing low-frequency and line noise, respectively. A visual inspection was then conducted on the continuous data of each participant to remove bad channels and visually identifiable artefacts. Blocks where the participants' error rate exceeded 35 % were also removed, as it was likely that the participant had responded to the incorrect target colour in these blocks. Across all three conditions and participants, 29 of 1440 blocks were excluded (2 %). 12, 11, and 6 blocks were removed in the Cloud, Lateral Target, and Central Target conditions, respectively. An extended Picard independent component analysis (ICA) was then performed across all 64 channels of the continuous data (61 EEG, 3 EOG; 500 steps, convergence bound = 1×10^{-7}), to remove components representing EOG and EKG artefacts prior to a back projection of the residuals. To check whether applying this ICA resulted in any substantial ERP differences relative to ERPs computed without ICA, probe N2pc waveforms obtained from data both with and without the ICA applied were compared. No systematic differences were obtained, and all statistical results were virtually identical for both sets of data. A 40 Hz low-pass FIR filter was then applied to remove high-frequency noise, followed by re-referencing of all EEG signals to the 61-channel common average. The data were then segmented relative to the onsets of the probe and search displays in each search condition, with each epoch including a 100 ms baseline prior to stimulus onset and the 400 ms thereafter. The epoched data were then submitted to an automatic, amplitude-based artefact rejection based on a generalized ESD test (OSL; https://ohba-analysis.github.io/), which removed 1.07 % (M = 86, SD = 80) of epochs across all participants. The per-condition ERP waveforms contralateral and ipsilateral to the location of the target colour in each probe and search display were then calculated at the lateral posterior electrodes PO7 and PO8, from which the respective N2pc component waveforms (the contralateral – ipsilateral difference wave) were derived.

A "smoothing" procedure (devised in Dodwell et al., 2024b) was then applied to the ERP and N2pc waveforms within each condition. This procedure improves the overall signal-to-noise ratio in RSPP probe data by averaging the waveforms of each set of three consecutive probes, centred on probe N ($N-1$, N, $N+1$). As a result, 26 newly "smoothed" ERP and N2pc waveforms were generated, centred on probes 2–27 (waveforms centred on probes 1 and 28 were not generated, as those probes lacked a preceding or subsequent probe, respectively). Within each condition, the mean and peak amplitudes of the smoothed waveforms were then calculated. Mean amplitudes were determined for both the ERP and N2pc waveforms, within an 80-ms window beginning 190 ms after stimulus onset. This N2pc time window was based on the 50 % onset and offset times of the N2pc waveforms elicited in a previous RSPP study (see Dodwell et al., 2024b). Peak amplitudes were only determined for the N2pc waveforms, within a 5-ms window + /- 2 ms from the most negative peak occurring within the N2pc time window.

3. Analysis

3.1. Behavioural analysis

The error rates (ERs) of each participant were first calculated for each block. Those blocks where the ER exceeded 35 % were removed from further analysis, while the ERs of the remaining blocks were averaged for each search condition. Participants' mean response times (RTs) were then calculated for each search condition, excluding trials with incorrect responses and those where the RTs were faster than 200 ms (which were considered anticipations) or slower than 1500 ms (which would have been input while the subsequent search display was being presented). The accumulated per-condition RTs and ERs of all participants were then submitted to separate one-way repeated measures ANOVAs, to assess any differential effects between each search

condition.

3.2. EEG analysis

Within each condition, EEG analysis was focused on determining if and at which probe latencies N2pc components were elicited. The smoothed ERP mean amplitudes identified for each condition were first submitted to a 2 × 26 repeated measures ANOVA, with factors of Laterality (contralateral vs ipsilateral to the target colour) and Probe Latency (probes 2–27). This was followed by pairwise Bayesian comparisons between the smoothed ERP mean amplitudes at each probe latency, to validate the presence or absence of the N2pc component on a per-probe basis. Cluster-based permutation analyses (N = 25,000, one-tailed, $\alpha = 0.05$) were also performed between the smoothed ERP waveforms of each probe latency, to cluster significantly more negative contralateral timepoints within the N2pc time window. This cluster-based permutation approach provides a convergent, non-parametric measure to determine the probability of differences between EEG time series (Maris & Oostenveld, 2007; or see Dodwell et al., 2024a for more detail).

Between conditions, EEG analysis was focused on identifying at which probe latencies activity within the N2pc time window differed. Within each pairing of conditions ("Cloud Target × Central Target", "Cloud Target × Lateral Target", and "Central Target × Lateral Target"), the smoothed N2pc mean and peak amplitudes were each submitted to a 2 × 26 repeated measures ANOVA, with factors of Condition (Condition A, Condition B of the given pair) and Probe Latency (probes 2–27). This was followed by pairwise Bayesian comparisons between the N2pc waveforms of each probe latency, to validate the presence of any per-probe differences. Cluster-based permutation analyses (N = 25,000, one-tailed, $\alpha = 0.05$) were also performed between the N2pc waveforms of each probe latency, clustering those timepoints within the N2pc time window that were significantly more negative in one condition as compared to the other. As a follow-up, the repeated-measures ANOVA and pairwise Bayesian comparisons indicated above were then repeated for each pairing of conditions across two subset ranges of probe latencies – namely, probes 20–23 and 24–27, as these ranges were shown to elicit N2pc components reliably and continuously within the "Cloud Target" condition.

4. Results

4.1. Behavioural results

The ANOVA of ERs did not indicate a main effect of condition ($F_{(2, 38)} = 0.68$, $p = .51$, $\eta_p^2 = 0.034$), demonstrating that mean error rates did not substantially differ between conditions (Cloud Target: $M = 5.36$ %, $SD = 3.92$ % | Central Target: $M = 4.71$ %, $SD = 4.37$ % | Lateral Target: $M = 5.30$ %, $SD = 4.43$ %). However, the ANOVA of RTs did detect a significant main effect of condition ($F_{(2, 38)} = 44.87$, $p < .001$, $\eta_p^2 = 0.702$), indicating that substantial differences were present between the mean response times in each condition (Cloud Target: $M = 387$ ms, $SD = 59$ ms | Central Target: $M = 362$ ms, $SD = 52$ ms | Lateral Target: $M = 400$ ms, $SD = 60$ ms). A set of follow-up pairwise comparisons confirmed that RTs were significantly faster in the Central Target condition as compared to either the Cloud Target condition ($t_{(19)} = -6.15$, $p_{bonf} < .001$, $d = -0.46$) or the Lateral Target condition ($t_{(19)} = -9.28$, $p_{bonf} < .001$, $d = -0.68$). Further, RTs in the Cloud Target condition were also significantly faster than in the Lateral Target condition ($t_{(19)} = -3.11$, $p_{bonf} = .017$, $d = -0.21$). As such, response times were shown to be fastest in the Central Target condition, moderate in the Cloud Target condition, and slowest in the Lateral Target condition.

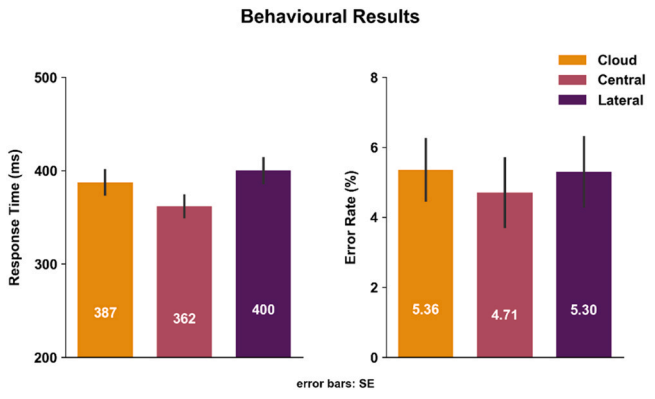

Fig. 2. Response Times (RTs) and Error Rates (ERs) to the search displays in the Cloud, Central, and Lateral Target task conditions. Although ERs did not significantly differ between the three conditions, RTs were shown to be fastest in the Central Target condition, moderate in the Cloud Target condition, and slowest in the Lateral Target condition.

4.2. EEG results

Probe N2pcs within each condition

Fig. 3 shows the smoothed lateralized difference waves from probes 2–27 in the Cloud Target condition. Reliable N2pc components were continuously elicited from probe 17 onwards (600 ms prior to search display onset), with steadily increasing magnitude towards the end of the preparation window. The ANOVA indicated a significant main effect of Laterality ($F_{(1, 19)} = 16.80$, $p = .001$, $\eta_p^2 = 0.47$), confirming that N2pcs had been elicited by the target-coloured probes. A significant Laterality × Probe Latency interaction was also indicated ($F_{(25, 475)} = 7.78$, $p < .001$, $\eta_p^2 = 0.29$), demonstrating that the magnitude of activity within the N2pc time window differed across the series of probe displays. The Bayesian pairwise comparisons revealed decisive evidence for the presence of N2pcs at probes 22–27 (all $BF_{10} \geq 152.38$, all $d \geq 0.40$), along with very strong evidence at probe 21 ($BF_{10} = 59.81$, $d = 0.50$), strong evidence at probe 20 ($BF_{10} = 20.83$, $d = 0.48$), and moderate evidence at probe 19 ($BF_{10} = 6.66$, $d = 0.38$). There was also strong evidence for the presence of contralateral negativity within the N2pc time window at probe 2 ($BF_{10} = 24.95$, $d = 0.10$), along with moderate evidence at probe 3 ($BF_{10} = 6.64$, $d = 0.10$). The results of the permutation analysis provided convergent confirmation of the Bayesian analysis, suggesting the presence of contralateral negativity within the N2pc time window of probe 17 and all other probes thereafter. The permutation analysis also detected significant clusters in probes 2–3.

Fig. 4 depicts the smoothed lateralized difference waves for probes 2–27 in the Central Target condition. N2pc components only appeared to be continuously elicited from probe 24 onwards (250 ms prior to search display onset), with magnitudes remaining relatively small approaching the end of the preparation window. A significant main effect of Laterality ($F_{(1, 19)} = 11.95$, $p = .003$, $\eta_p^2 = 0.39$) was indicated by the ANOVA, again demonstrating that N2pcs had indeed been elicited by the target-coloured probes. A significant Laterality × Probe Latency interaction was also detected ($F_{(25, 475)} = 2.14$, $p = .001$, $\eta_p^2 = 0.10$), indicating differing magnitudes of activity within the N2pc time window across probe displays. Bayesian pairwise comparisons showed decisive evidence for the presence of an N2pc at probe 26 ($BF_{10} = 125.40$, $d = 0.40$), strong evidence at probe 25 ($BF_{10} = 25.01$, $d = 0.30$), and moderate evidence at probes 24 ($BF_{10} = 3.98$, $d = 0.21$) and 27 ($BF_{10} = 8.96$, $d = 0.12$). Very strong evidence for the presence of contralateral negativity within the N2pc time window was also indicated at probe 8 ($BF_{10} = 30.46$, $d = 0.08$). Permutation analyses generally complemented the Bayesian findings, suggesting the presence of contralateral negativity within the N2pc time window for probes 25, 26, and 27, although no cluster was indicated for probe 26. The permutation analysis also indicated a significant cluster of contralateral negativity at probe 8.

Fig. 5 provides the smoothed lateralized difference waves of probes 2–27 in the Lateral Target condition. Similar to the Central Target

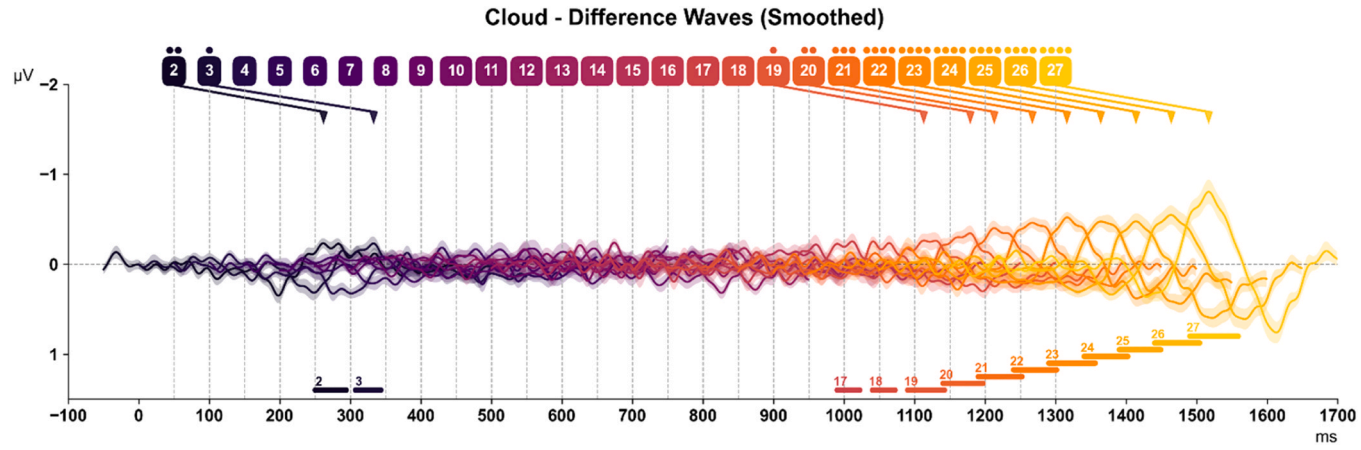

Fig. 3. Lateralized difference waves (contralateral – ipsilateral waveforms over scalp sites PO7/PO8) elicited by the 28 consecutive probe displays in the "Cloud Target" condition, "smoothed" via averaging across each set of three successive waveforms centred on probe N (N-1, N, N + 1). The latency of each probe onset is indicated by a vertical dashed line adjoining a uniquely coloured and numbered label above. The smoothed waveforms relative to each probe latency appear in the same colour as their corresponding label, beginning 100 ms prior to their respective onset and then continuing for 400 ms thereafter. The waveforms of all probes overlap within the figure but are also spaced in accordance with their temporal occurrence. The waveforms for which pairwise Bayesian analysis demonstrated substantial contralateral negativity within the N2pc time window (190–270 ms after probe onset) are demarcated by dots appearing above their respective latency labels and in their corresponding colour (• = $BF_{10} > 3$, •• = $BF_{10} > 10$, ••• = $BF_{10} > 30$, •••• = $BF_{10} > 100$) along with an arrow over their respective peak. The portions of each waveform wherein permutation analysis detected significant clusters of contralateral negativities within the N2pc time window are marked below with correspondingly coloured and numbered horizontal bars.

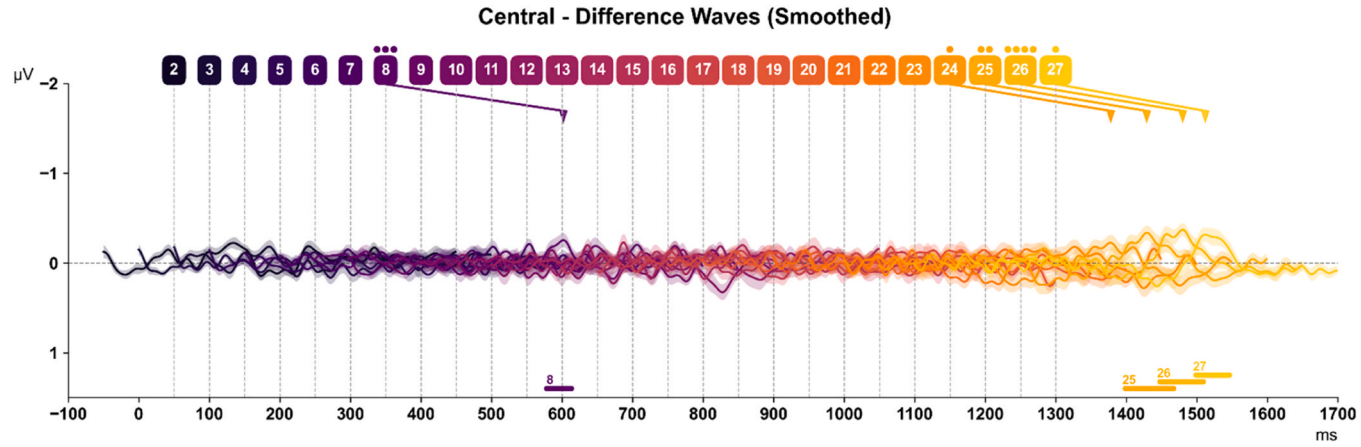

Fig. 4. Smoothed lateralized difference waves elicited in the Central Target condition. The structure and layout of Fig. 4 is otherwise identical to that of Fig. 3.

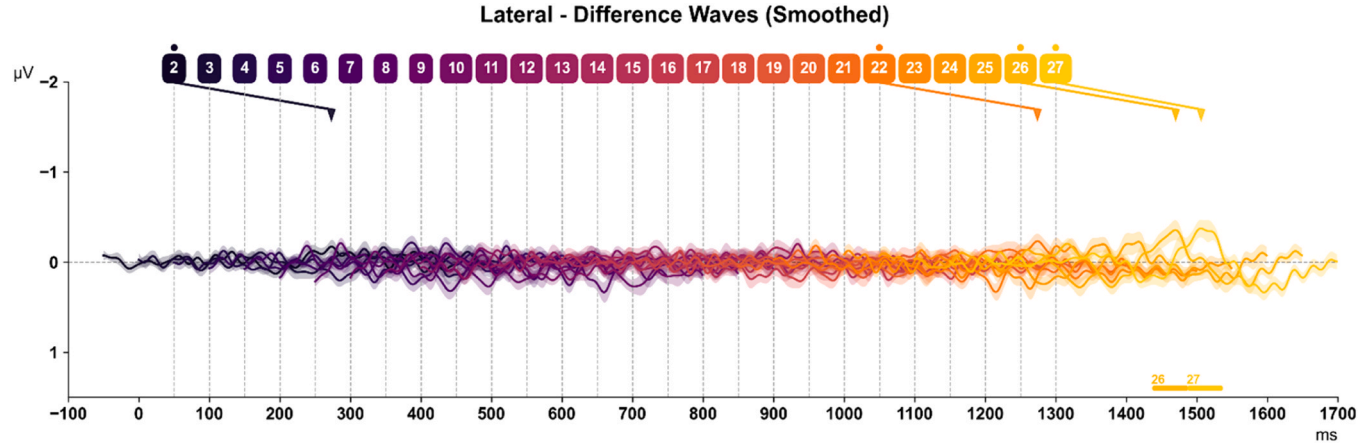

Fig. 5. Smoothed lateralized difference waves elicited in the Lateral Target condition. The structure and layout of Fig. 5 is otherwise identical to that of Figs. 3 and 4.

condition, N2pc components were only consistently elicited near the end of the preparation window, from probe 26 onwards (100 ms prior to search display onset). The ANOVA results revealed a significant main effect of Laterality ($F_{(1, 19)} = 4.39$, $p = .050$, $\eta_p^2 = 0.19$), validating the presence of N2pcs to target-coloured probes. However, no Laterality × Probe Latency interaction was found ($p = .080$). Further, Bayesian pairwise analyses only detected moderate evidence for the presence of N2pcs at probes 22, 26, and 27 (all $BF_{10} \geq 6.80$, all $d \geq 0.11$), with additional moderate evidence for contralateral negativity at probe 2 ($BF_{10} = 5.24$, $d = 0.06$). Similarly, permutation analysis only revealed significant clusters of contralateral negativities suggesting the presence of N2pcs at probes 26 and 27.

Interactive versions of Fig. 3, Fig. 4, and Fig. 5 can be found at the following URL: https://gordondodwell.github.io/RSPPHD_Spatial_Results/

4.3. Comparisons of probe N2pcs between paired conditions

Fig. 6 displays a comparison between the smoothed lateralized difference waves of probes 2–27 in the Cloud Target and Central Target conditions. Differences between these two conditions were apparent from around probe 20 onwards, with N2pc waveforms in the Cloud Target condition appearing to emerge substantially earlier and with greater magnitudes than in the Central Target condition. Accordingly, the ANOVA results revealed a significant main effect of Condition ($F_{(1, 19)} = 6.05$, $p = .024$, $\eta_p^2 = 0.24$), confirming that the magnitude of activity within the N2pc time window differed between the two conditions. A significant Condition × Probe Latency interaction was also observed ($F_{(1, 19)} = 2.21$, $p = .001$, $\eta_p^2 = 0.10$), suggesting that the presence or absence of these differences varied across probes. Bayesian pairwise comparisons between the mean amplitudes of each condition provided strong evidence for more substantial negativities in the Cloud Target condition at probes 23 ($BF_{10} = 13.05$, $d = 0.88$) and 27 ($BF_{10} = 10.49$, $d = 0.96$), along with moderate evidence at probe 22 ($BF_{10} = 4.42$, $d = 0.91$). Correspondingly, Bayesian comparisons between the peak amplitudes of each condition provided very strong evidence for a more negative peak in the Cloud Target condition at probe 27 ($BF_{10} = 32.05$, $d = 0.95$), along with strong evidence at probe 22 ($BF_{10} = 26.63$, $d = 1.14$), and moderate evidence at probe 23 ($BF_{10} = 8.18$, $d = 0.83$). The permutation analysis was somewhat more sensitive to differences in the magnitude of negativities between each condition, resulting in significant clusters at probes 21–24, 26, and 27 wherein the waveforms of the Cloud Target condition were shown to be substantially more negative.

A comparison between the smoothed lateralized difference waves of probes 2–27 in the Cloud Target and Lateral Target conditions is depicted in Fig. 7. Differences between these two conditions were again visible from approximately probe 20 onwards, with the Cloud Target condition eliciting earlier and more substantial N2pc waveforms. The ANOVA results again confirmed this observation, revealing a significant main effect of Condition ($F_{(1, 19)} = 8.72$, $p = .008$, $\eta_p^2 = 0.32$) along with a significant Condition × Probe Latency interaction ($F_{(1, 19)} = 2.39$, $p < .001$, $\eta_p^2 = 0.11$), demonstrating probe-dependent differences in N2pc magnitudes between the two conditions. Bayesian pairwise comparisons between the mean amplitudes of each condition provided decisive evidence for greater negativity in the Cloud Target condition at probe 27 ($BF_{10} = 147.51$, $d = 1.03$), along with very strong evidence at probe 23 ($BF_{10} = 93.29$, $d = 1.21$), strong evidence at probe 22 ($BF_{10} = 24.53$, $d = 1.01$), and moderate evidence at probes 24 and 25 (all $BF_{10} \geq 3.39$, all $d \geq 0.59$). Bayesian comparisons between the peak amplitudes were somewhat less sensitive, indicating strong evidence for a more negative peak in the Cloud Target condition at probe 27 ($BF_{10} = 52.31$, $d = 0.80$), but otherwise only moderate evidence at probes 22 and 23 (all $BF_{10} \geq 3.04$, all $d \geq 0.56$). The permutation analysis was again more sensitive to differences overall, indicating clusters of greater negativities in the Cloud Target condition across probes 20, 22–25, and 27.

Fig. 8 compares the smoothed lateralized difference waves of probes 2–27 in the Central Target and Lateral Target conditions. Little to no differences were apparent between these two conditions. This was confirmed by the ANOVA results, which did not demonstrate a main effect of Condition ($p = .317$) or any Condition × Probe Latency interaction ($p = .638$). As such, no evidence was provided to suggest that activity within the N2pc window differed between the Central Target and Lateral Target conditions at any probe latency. Further, Bayesian pairwise comparisons between both the mean and peak amplitudes of the two conditions did not reveal any reliable evidence for differences at any probe latency (all $BF_{10} \geq 0.23$ but ≤ 2.61). As final demonstration of their similarity, permutation analysis also failed to detect any clusters of

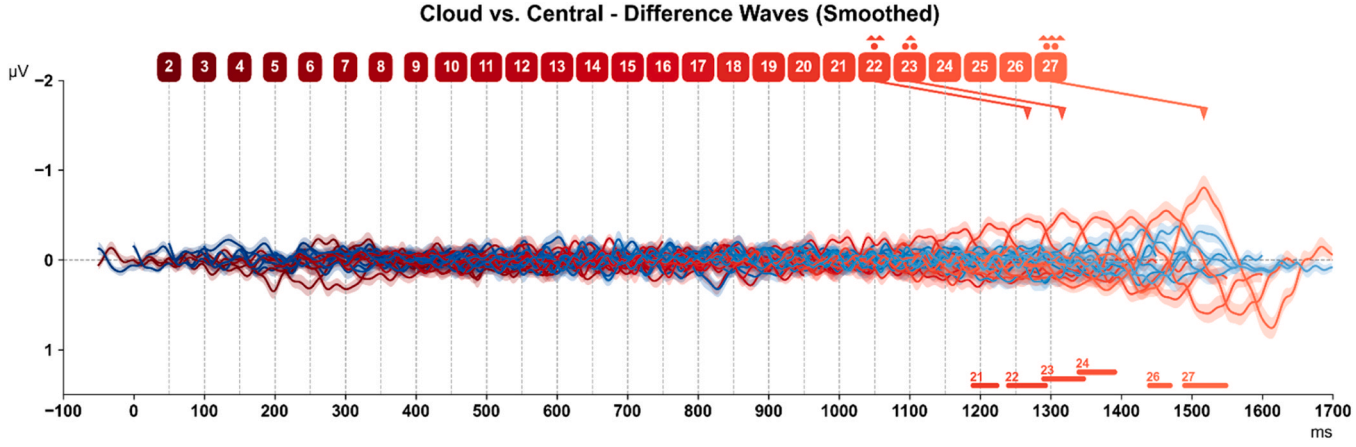

Fig. 6. Comparison of the smoothed lateralized difference waves elicited in the Cloud Target and Central Target conditions. The structure of Figs. 6–8 is generally similar to that of Figs. 3–5; however, each probe label and relative onset is shared by a pair of smoothed waveforms from each condition. The waveforms of the Cloud Target condition and the corresponding probe latency labels appear in shades of red, while the waveforms of the Central Target condition are shown in shades of blue. The probe latencies for which Bayesian pairwise analyses indicated mean amplitudes within the N2pc time window to be substantially more negative in one condition as compared to the other are demarcated by dots appearing above the corresponding label and in the respective colour (• = $BF_{10} > 3$, •• = $BF_{10} > 10$, ••• = $BF_{10} > 30$, •••• = $BF_{10} > 100$). Similarly, those for which Bayesian pairwise analyses indicated the peak magnitudes as being substantially more negative are demarcated above the corresponding label and in the respective colour by triangles (^ = $BF_{10} > 3$, ^^ = $BF_{10} > 10$, ^^^ = $BF_{10} > 30$, ^^^^ = $BF_{10} > 100$). The portions of each pair of waveforms wherein permutation analyses detected clusters of significantly more negative activity within one condition as compared to the other are also marked below via correspondingly coloured and numbered horizontal bars.

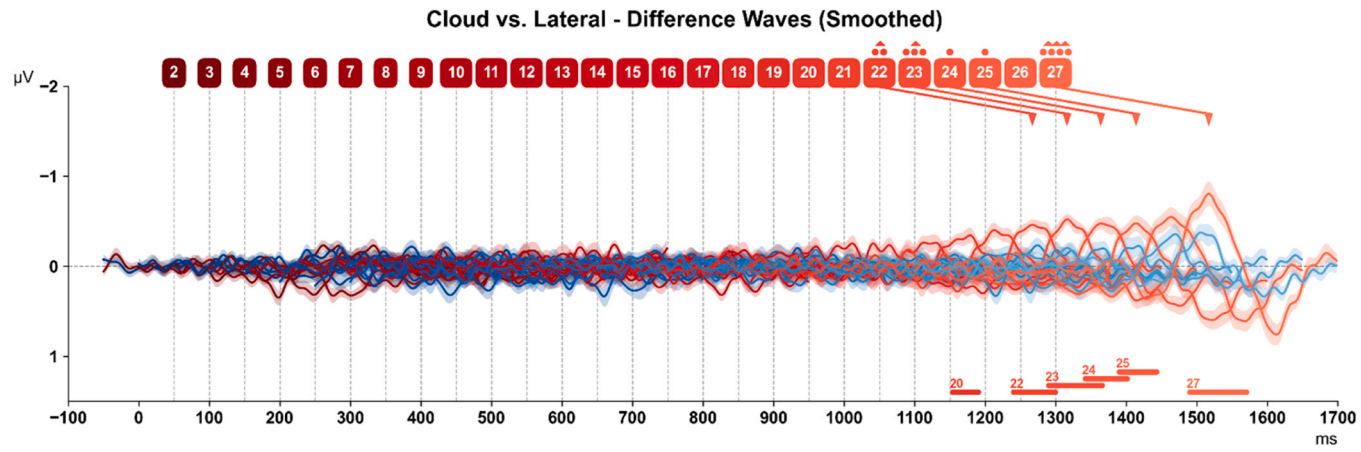

Fig. 7. Comparison of the smoothed lateralized difference waves in the Cloud Target and Lateral Target conditions. The structure and layout of Fig. 7 is otherwise identical to that of Fig. 6.

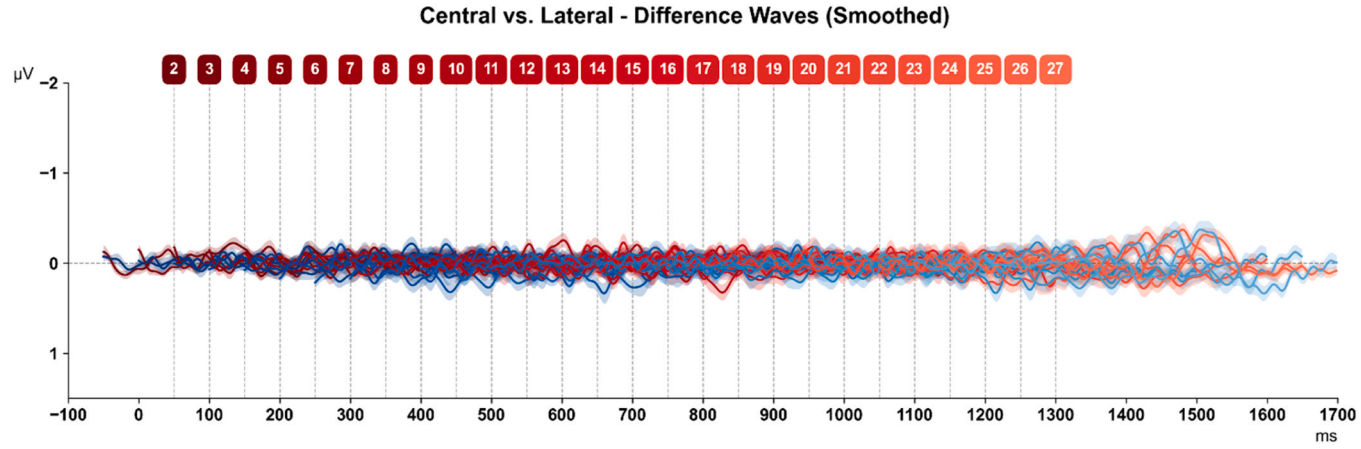

Fig. 8. Comparison of the smoothed lateralized difference waves in the Central Target and Lateral Target conditions. The structure and format of Fig. 8 is otherwise identical to that of Figs. 7 and 6.

differences between the two conditions.

5. Discussion

The guidance of visual search is controlled by target templates which represent attributes relevant for finding target objects, and are activated in a preparatory fashion prior to the start of search episodes (Desimone & Duncan, 1995; Olivers et al., 2011; Eimer, 2014; Grubert & Eimer, 2018). Attentional templates represent non-spatial target features, such as colour, size, or shape, but it remains unknown whether information about *where* targets can appear in the visual field can also be represented during search preparation. When observers selectively prepare for known target features, can they restrict this selectivity to areas of the visual field that are relevant for an upcoming search task? This should be possible if the spread of feature-based attention can be controlled by spatial filtering, but not if it always operates in a spatially global fashion across the entire visual field.

The present study tracked the preparatory activation of colour-specific target templates by measuring N2pc components in response to probe displays composed of lateralised 'clouds' of coloured dots, in which a target-matching colour would appear in a lateralised position. These probe displays were presented in rapid succession, appearing every 50 ms during a 1600 ms interval between successive search displays, and participants were instructed to find and localize a colour-defined target item. This procedure was repeated across three separate task conditions. In the Cloud Target condition, targets appeared in the same locations as the preceding cloud probes, thereby rendering the probed locations task-relevant. In the two other conditions, the targets always appeared at different locations (Central Target: around fixation; Lateral Target: in the vacant centre of either cloud), so that the locations of the cloud probes were task-irrelevant. The critical question was whether this manipulation of search target locations would affect the pattern of N2pc components in response to physically identical cloud probe displays. If preparatory attentional templates only represent non-spatial target features in a spatially global fashion, no probe N2pc differences should be found between these three conditions. Alternatively, if these preparatory states are sensitive to information about target locations, systematic probe N2pc differences should be found between the Cloud Target condition and the two other conditions.

The N2pc results observed in the Cloud Target condition confirmed the findings of our previous study that employed the same task (Dodwell et al., 2024b), as well as earlier experiments that used different probe procedures (e.g., Grubert & Eimer, 2018; Dodwell et al., 2024a). Reliable probe N2pcs emerged contralateral to target-colour probes from about 600 ms prior to search display onset, and were maximal in response to the probe that immediately preceded the upcoming search display (see Fig. 3). These observations were confirmed by standard statistical methods (ANOVAs and t-tests) and also by Bayesian and cluster-based permutation analyses. These observations show that reliable probe N2pcs could be extracted even though probe displays were presented in rapid succession, which inevitably results in temporally overlapping ERPs. Lateralised responses triggered by target-colour dots

for individual bilateral cloud displays could be computed because each individual probe display was equally likely to be preceded and followed by a display where target-colour dots were presented on the same or the opposite side. The subtraction of ipsilateral from contralateral ERPs for each probe display therefore only reflects lateralised activity elicited by this display, without any overlap of lateralised responses to the previous or subsequent display.

Critically, the N2pc results obtained in the Central and Lateral Target task were systematically different. Relative to the Cloud Target task, reliable N2pc components emerged later during the preparation period and were smaller in size immediately prior to search display onset. These differences, which were confirmed by pairwise comparisons between tasks, demonstrate that the task-relevance of probe locations had a clear impact on the activation profiles of colour-selective target templates during search preparation. These N2pc results show that, at least in tasks where search targets always appear within particular regions of the visual field, search preparation processes are sensitive to this spatial information about task-relevant and irrelevant locations. In this context, the difference in the size of the search displays between the Cloud Target and the other two tasks may be relevant, as this difference may have affected not just the locus, but also the size of the spatial focus of attention during the preparation period. A more narrow attentional focus may have resulted in smaller overall feature-based modulations of target-colour probe processing, resulting in smaller N2pc components relative to the Cloud Target task.

It should be noted that the delay of probe N2pcs in the Central and Lateral Target tasks relative to the Cloud Target Task may have been associated with the attenuation of N2pc amplitudes in these two tasks. Given the limitations imposed by signal-to-noise ratios, smaller N2pc components will be detectable relatively late during the preparation period, close to the presentation of the next search display, whereas larger N2pcs can be reliably measured at an earlier point in time. More importantly, the fact remains that task-dependent probe N2pc differences were clearly present. This suggests that although preparatory search templates represent information about target-defining non-spatial features, they do not always operate in an entirely unrestrained spatially global fashion. This is in line with previous research demonstrating that feature-based attention can be subject to spatial filtering (e.g., Andersen et al., 2011; Leonard et al., 2015; Berggren & Eimer, 2020). The delayed onset of probe N2pc components in the two tasks where probes appeared at irrelevant locations is also consistent with the observation in a recent SSVEP experiment (Andersen & Hillyard, 2024) that feature-based attentional effects emerge about 150 ms later on the unattended side of the visual field. However, these effects were measured during task performance and not during task preparation, as in the present study. Importantly, the current observations suggest that such spatial filtering processes do not completely eliminate feature-based attentional modulations at task-irrelevant locations during search preparation. Even though probe-induced N2pc components were attenuated and emerged later in the Central and Lateral Target tasks relative to the Cloud Target task, they remained reliably present during the final phase of the preparation period (from about 200 ms prior to search display presentation). In other words, feature-based attentional modulations were reduced in size at known task-irrelevant locations, but they were not entirely abolished.

These observations suggest that during search preparation, feature-based attention is at least in part decoupled from focal spatial attention, and continues to operate at spatially unattended locations even when these locations can be completely ignored for an extended period (i.e., several consecutive experimental blocks). Perhaps the strongest demonstration of this partial independence of feature-based and space-based attention comes from the observation that clear feature-based attention effects were found in response to lateral target-colour probes in the Central Target task, where spatial selectivity should have been relatively straightforward. When attention can be tightly focused around central fixation, it should not be very challenging to filter out visual signals from more peripheral areas before feature-based attentional modulations can emerge. The presence of reliable N2pcs to target-colour probes from about 250 ms prior to search display onset demonstrates that even under these conditions, some spatially global monitoring of peripheral visual input for task relevance remained during search preparation. This observation may not be as surprising as it first appears. In more naturalistic contexts, unattended peripheral information may never be completely irrelevant, as some potentially important event may suddenly appear unexpectedly. In addition, even looked-for target objects may sometimes occur at unexpected locations. For these reasons, it may be adaptive for feature-based attention to retain some degree of independence from top-down spatial filtering under all circumstances, even when preparing and performing attentional selection tasks at a particular location (see also Smout, Garrido, & Mattingley, 2020, for ERP evidence that surprising stimuli at irrelevant locations elicit strong feature-based attentional responses).

On the other hand, as described earlier, spatial filtering clearly played an important role in modulating the magnitude of feature-based attentional modulations in the present study. This is particularly notable in the Lateral Target task, which was designed to make any spatially selective processing of task-relevant versus irrelevant locations very challenging. Because search targets unpredictably appeared in the left or right hemifield, within the central empty area of one of the two clouds, both of these areas had to be attended simultaneously. The observation that probe N2pcs in this task were reliably attenuated relative to the Cloud Target task shows that some spatial selectivity still emerged, reducing the ability of template-matching probes to attract attention. This suggests that observers were able to focus attention to some degree on the two task-relevant locations, while excluding the surrounding larger areas which contained the cloud probes. The fact there were no probe N2pc differences between the Central and Lateral Target tasks indicates spatial filtering was similarly efficient when attention was focused on a single foveal region or on two spatially distinct regions in the left and right visual field.

We have attributed the differences between target-colour template activation processes reflected by probe N2pc components in the Cloud Target condition and the other two conditions to the spatial filtering of feature-based attention. However, there is the theoretical possibility that target-colour templates were generally activated more strongly and earlier in the Cloud Target condition, resulting in larger N2pc components. Still, it is not clear why colour-specific search preparation should have been much more pronounced in the Cloud Target condition, and the behavioural results provide no evidence that search in this condition was substantially harder than in the other two. RTs in the Cloud Target condition were slightly slower than in the Central Target condition, but faster than in the Lateral Target condition, and there were no differences between conditions in error rates. One clear difference between the Cloud Target and the other two conditions was that search displays looked very different and occupied a much larger area (see Fig. 1), which might have inadvertently resulted in stronger preparatory template activation. However, several previous experiments from our lab which tracked search template activation processes with probe N2pcs (e.g., Grubert & Eimer, 2018, 2019, 2020) employed search displays more similar to those used here in the Lateral and Central Target tasks than to that of the Cloud Target task. All these experiments found a pattern of probe N2pcs similar to that observed here for the Cloud Target task. Thus, the possibility that search display differences resulted in differential search template activation between tasks can be ruled out (see also Dodwell et al., 2024a, for evidence that a similar pattern is elicited during task preparation even when task-relevant displays contain a single target object without distractors). These considerations strongly suggest that the difference of probe N2pcs between tasks does not reflect generic differences in search template activation, but rather the effects of spatial filtering, which attenuate feature-based attentional modulations at task-irrelevant locations.

Overall, the current results have shed new light on interactions

between space-based and feature-based attentional control processes during the preparation for particular search episodes. Knowledge about the locations at which task-relevant stimuli will appear modulates visual processing already prior to the arrival of search displays. This shows that spatial expectations (space-based templates) can modulate the effects of feature-based templates, and that feature-based attention does not operate in a completely spatially global fashion during search preparation. However, feature-based attentional selectivity was not completely eliminated at task-irrelevant locations, suggesting that even when upcoming target locations are fully predictable, some feature-selective monitoring continues to occur across the entire visual field.

Funding Information

This work was supported by the Economic and Social Research Council (ESRC; grant reference ES/V002708/1).

Open Access Statement

For the purposes of open access, the author has applied a creative commons attribution (CC BY) licence to any author accepted manuscript version arising.

CRediT authorship contribution statement

Nako Rebecca: Resources, Project administration, Funding acquisition. **Dodwell Gordon:** Writing – review & editing, Writing – original draft, Visualization, Validation, Software, Methodology, Investigation, Formal analysis, Data curation, Conceptualization. **Eimer Martin:** Writing – review & editing, Writing – original draft, Supervision, Resources, Project administration, Methodology, Funding acquisition, Conceptualization.

Declaration of Generative AI and AI-assisted technologies in the writing process

The authors have not employed any form of generative AI or AI-assisted technologies in the writing of this manuscript.

Declaration of Competing Interest

The authors declare that they have no known competing financial interests or personal relationships that could have appeared to influence the work reported in this paper.

Data availability

A Link to a repository containing the raw data and analysis scripts has been included in the body of the manuscript and at the attach file step of the submission process.

EEG evidence for spatial selectivity in feature-based preparation for visual search (OSF)

References

Andersen, S. K., Fuchs, S., & Müller, M. M. (2011). Effects of feature-selective and spatial attention at different stages of visual processing. *Journal of Cognitive Neuroscience, 23*(1), 238–246. https://doi.org/10.1162/jocn.2009.21328

Andersen, S. K., & Hillyard, S. A. (2024). The time course of feature-selective attention inside and outside the focus of spatial attention. *Proceedings of the National Academy of Sciences, 121*(16), Article e2309975121.

Andersen, S. K., Hillyard, S. A., & Müller, M. M. (2013). Global facilitation of attended features is obligatory and restricts divided attention. *Journal of Neuroscience, 33*(46), 18200–18207. https://doi.org/10.1523/JNEUROSCI.1913-13.2013

Berggren, N., & Eimer, M. (2020). Spatial filtering restricts the attentional window during both singleton and feature-based visual search. *Attention, Perception, Psychophysics, 82*, 2360–2378. https://doi.org/10.3758/s13414-020-01977-5

Bichot, N. P., Rossi, A. F., & Desimone, R. (2005). Parallel and serial neural mechanisms for visual search in macaque area V4. *Science, 308*(5721), 529–534. https://doi.org/10.1126/science.1109676

Desimone, R., & Duncan, J. (1995). Neural mechanisms of selective visual attention. *Annual Review of Neuroscience, 18*, 193–222. https://doi.org/10.1146/annurev.ne.18.030195.001205

Dodwell, G., Nako, R., & Eimer, M. (2024a). The Preparatory Activation of Guidance Templates for Visual Search and of Target Templates in Non-Search Tasks. *Journal of Cognition, 7*(1). https://doi.org/10.5334/joc.341

Dodwell, G., Nako, R., & Eimer, M. (2024b). A new method for tracking the preparatory activation of target templates for visual search with high temporal precision. *Psychophysiology*. , Article e14582. https://doi.org/10.1111/psyp.14582

Duncan, J., & Humphreys, G. W. (1989). Visual search and stimulus similarity. *Psychological Review, 96*, 433. https://doi.org/10.1037/0033-295X.96.3.433

Eimer, M. (1996). The N2pc component as an indicator of attentional selectivity. *Electroencephalography and Clinical Neurophysiology, 99*, 225–234. https://doi.org/10.1016/0013-4694(96)95711-9

Eimer, M. (2014). The neural basis of attentional control in visual search. *Trends in Cognitive Sciences, 18*, 526–535. https://doi.org/10.1016/j.tics.2014.05.005

Eimer, M. (2015). EPS Mid-Career Award 2014: The control of attention in visual search: Cognitive and neural mechanisms. *Quarterly Journal of Experimental Psychology, 68*(12), 2437–2463. https://doi.org/10.1080/17470218.2015.1065283

Eimer, M., & Kiss, M. (2008). Involuntary attentional capture is determined by task set: Evidence from event-related brain potentials. *Journal of Cognitive Neuroscience, 20*(8), 1423–1433. https://doi.org/10.1162/jocn.2008.20099

Faul, F., Erdfelder, E., Lang, A. G., & Buchner, A. (2007). G*Power 3: A flexible statistical power analysis program for the social, behavioral, and biomedical sciences. *Behavioural Research Methods, 39*, 175–191. https://doi.org/10.3758/BF03193146

Folk, C. L., Remington, R. W., & Johnston, J. C. (1992). Involuntary covert orienting is contingent on attentional control settings. *Journal of Experimental Psychology: Human Perception and Performance, 18*(4), 1030–1044. https://doi.org/10.1037/0096-1523.18.4.1030

Forschack, N., Andersen, S. K., & Müller, M. M. (2017). Global enhancement but local suppression in feature-based attention. *Journal of Cognitive Neuroscience, 29*(4), 619–627. https://doi.org/10.1162/jocn_a_01075

Gramfort, A., Luessi, M., Larson, E., Engemann, D. A., Strohmeier, D., Brodbeck, C., & Hämäläinen, M. (2013). MEG and EEG data analysis with MNE-Python. *Frontiers in Neuroinformatics, 7*, 267. https://doi.org/10.3389/fnins.2013.00267

Grubert, A., & Eimer, M. (2020). Preparatory template activation during search for alternating targets. *Journal of Cognitive Neuroscience, 32*(8), 1525–1535. https://doi.org/10.1162/jocn_a_01565

Grubert, A., & Eimer, M. (2018). The time course of target template activation processes during preparation for visual search. *Journal of Neuroscience, 38*, 9527–9539. https://doi.org/10.1523/JNEUROSCI.0409-18.2018

Grubert, A., & Eimer, M. (2019). Concurrent attentional template activation during preparation for multiple-colour search, 233-233 *Journal of Vision, 19*(10). https://doi.org/10.1167/19.10.233.

Hickey, C., Di Lollo, V., & McDonald, J. J. (2009). Electrophysiological indices of target and distractor processing in visual search. *Journal of Cognitive Neuroscience, 21*(4), 760–775. https://doi.org/10.1162/jocn.2009.21039

Leonard, C. J., Balestreri, A., & Luck, S. J. (2015). Interactions between space-based and feature-based attention. *Journal of Experimental Psychology: Human Perception and Performance, 41*(1), 11. https://doi.org/10.1037/xhp0000011

Liu, T. (2019). Feature-based attention: effects and control. *Current Opinion in Psychology, 29*, 187–192. https://doi.org/10.1016/j.copsyc.2019.03.013

Luck, S. J., & Hillyard, S. A. (1994). Spatial filtering during visual search: Evidence from human electrophysiology. *Journal of Experimental Psychology: Human Perception and Performance, 20*, 1000–1014. https://doi.org/10.1037/0096-1523.20.5.1000

Maris, E., & Oostenveld, R. (2007). Nonparametric statistical testing of EEG-and MEG-data. *Journal of Neuroscience Methods, 164*, 177–190. https://doi.org/10.1016/j.jneumeth.2007.03.024

Martinez-Trujillo, J. C., & Treue, S. (2004). Feature-based attention increases the selectivity of population responses in primate visual cortex. *Current Biology, 14*(9), 744–751. https://doi.org/10.1016/j.cub.2004.04.028

Olivers, C. N., Peters, J., Houtkamp, R., & Roelfsema, P. R. (2011). Different states in visual working memory: When it guides attention and when it does not. *Trends in Cognitive Sciences, 15*(7), 327–334. https://doi.org/10.1016/j.tics.2011.05.004

Peirce, J. W., Gray, J. R., Simpson, S., MacAskill, M., Höchenberger, R., Sogo, H., Kastman, E., & Lindeløv, J. K. (2019). PsychoPy2: Experiments in behavior made easy. *Behavior Research Methods, 51*, 195–203. https://doi.org/10.3758/s13428-018-01193-y

Re, D., Inbar, M., Richter, C. G., & Landau, A. N. (2019). Feature-based attention samples stimuli rhythmically. *Current Biology, 29*(4), 693–699. https://doi.org/10.1016/j.cub.2019.01.010

Serences, J. T., & Boynton, G. M. (2007). Feature-based attentional modulations in the absence of direct visual stimulation. *Neuron, 55*(2), 301–312. https://doi.org/10.1016/j.neuron.2007.06.015

Smout, C. A., Garrido, M. I., & Mattingley, J. B. (2020). Global effects of feature-based attention depend on surprise. *NeuroImage, 215*, Article 116785. https://doi.org/10.1016/j.neuroimage.2020.116785

Störmer, V. S., & Alvarez, G. A. (2014). Feature-based attention elicits surround suppression in feature space. *Current Biology, 24*(17), 1985–1988. https://doi.org/10.1016/j.cub.2014.07.030

Theeuwes, J. (2010). Top–down and bottom–up control of visual selection. *Acta Psychologica, 135*(2), 77–99. https://doi.org/10.1016/j.actpsy.2010.02.006

Theeuwes, J., Kramer, A. F., & Atchley, P. (2001). Spatial attention in early vision. *Acta Psychologica, 108*(1), 1–20. https://doi.org/10.1016/s0001-6918(00)00066-4

Wolfe, J. M. (2021). Guided Search 6.0: An updated model of visual search. *Psychonomic Bulletin Review, 28*, 1060–1092. https://doi.org/10.3758/s13423-020-01859-9

Woodman, G. F., & Luck, S. J. (1999). Electrophysiological measurement of rapid shifts of attention during visual search. *Nature, 400*, 867–869. https://doi.org/10.1038/23698

Yantis, S., & Jonides, J. (1990). Abrupt visual onsets and selective attention: voluntary versus automatic allocation. *Journal of Experimental Psychology: Human Perception and Performance, 16*(1), 121. https://doi.org/10.1037/0096-1523.16.1.121

Zhang, W., & Luck, S. J. (2011). The number and quality of representations in working memory. *Psychological Science, 22*(11), 1434–1441. https://doi.org/10.1177/0956797611417006